Available online at www.sciencedirect.com
ScienceDirect
Catalysis Today 125 (2007) 81–87
CATALYSIS TODAY
www.elsevier.com/locate/cattod

Selective methanation of carbon oxides in a microchannel reactor—Primary screening and impact of gas additives

Yong Men *, Gunther Kolb, Ralf Zapf, Volker Hessel, Holger Löwe

Institut für Mikrotechnik Mainz GmbH, Chemical Process Technology, Carl-Zeiss-Str. 18-20, D-55129 Mainz, Germany

Available online 26 March 2007

Abstract

Selective removal of CO by methanation of carbon oxides has been performed over wash-coated supported metal catalysts in a microchannel reactor with simulated reformate feeding. The primary screening over a series of Ru and Ni-based catalysts shows that methanation activity is markedly dependent on the type of metal, the metal loadings and the promoter. $Ni/CaO/Al_2O_3$ catalyst exhibits the highest methanation activity with CO conversion higher than 93% and a relatively low conversion of CO_2 into methane among investigated catalysts at 300 °C under the operating condition. The appropriate temperature for selective methanation was identified to be 250 °C below which CO methanation preferentially and exclusively occurs. The effect of reaction temperature and gas additives such as steam and gaseous oxygen on the methanation performance is presented in terms of catalytic activity, selectivity, and methane yield. The regulation of carbon oxides methanation on $Ni/CaO/Al_2O_3$ catalyst by gaseous oxygen was realized by a switchover of the reaction pathway from combustion reaction in the presence of gas phase oxygen to the methanation upon the complete consumption of oxygen and the dynamic behaviour of catalyst surface induced by the interplay of the catalyst surface and the gas phase reactants.

Keywords: Microchannel reactor; Methanation; Heterogeneous catalysis; CO removal; Hydrogen purification

1. Introduction

Future energy generation for stationary, distributed and mobile applications will be based to a significant extent upon fuel cell technology [1]. The most promising fuel-cell technology for transport applications appears to be the Polymer Electrolyte Membrane Fuel Cell (PEMFC) fueled by hydrogen. Hydrogen powered fuel cells are expected to become important energy carriers for sustained energy consumption with reduced impact on the environment [2]. However, hydrogen fuel cells present obvious problems with generation, storage, and distribution. Pressurized vessels or metal hydrides in a vehicle occupy space, increase weight, and decrease fuel efficiency. As a result, attention has been focused on the conversion of more readily available fuels to hydrogen, either on board of a vehicle [3] or at a service station. The conversion of hydrocarbons and alcohols may be achieved by catalytic reforming or by partial oxidation [4]. In the short to medium term, fuel processing will play a significant role in hydrogen production for fuel cell applications, because the already existing distribution network to supply the consumer with fossil fuels will support the introduction of fuel cell technology onto the market place. One of the major problems for the introduction of low temperature PEMFC as the power source for electrically operated vehicles is the delivery of ''nearly-CO-free'' feed gas, which becomes problematic whenever H_2 is generated from fuels such as methanol or gasoline, as the fuel cell anodes can be poisoned even by trace impurities of CO. As a consequence, it is essential to reduce CO content to the level below 50 ppm for state-of-art PtRu anode electrocatalysts, and, preferably, below 10 ppm for Pt anode electrocatalysts [5].

Theoretically, there are several methods to reduce carbon monoxide to the levels acceptable for a fuel cell [6]. It is feasible to separate hydrogen by diffusion through a CO filtering membrane [7] but the membrane is expensive and it usually requires a compressor owing to high pressure. The most studied system for the removal of final traces of CO has been the selective oxidation of CO in a H_2-rich atmosphere (PROX)

* Corresponding author. Tel.: +49 6131 990 441; fax: +49 6131 990 205.
E-mail address: men@imm-mainz.de (Y. Men).

0920-5861/$ – see front matter © 2007 Elsevier B.V. All rights reserved.
doi:10.1016/j.cattod.2007.02.017

over the last years since it has the ability to remove CO down to 10 ppm [8–10]. The catalytic hydrogenation of carbon monoxide and carbon dioxide also produces a large variety of products ranging from methane and methanol to higher molecular weight hydrocarbons and alcohols [11,12]. The methanation of CO and CO_2 as well as the related Fischer–Tropsch reaction have been extensively studied and reviewed. CO_x methanation may have another practical application as a means of CO removal from process gases for gas separation purposes and is also being discussed as an alternative to PROX in fuel processors for mobile fuel cell applications. Recently, selective methanation of carbon monoxide has emerged as a promising route to remove CO in the reformate stream down to 20 ppm for the use of polymer electrolyte fuel cells [13,14].

Microchannel reactors have been employed to minimize the complicated chemical plants mainly due to their advantages for chemical reactions such as several orders of magnitude higher surface to volume ratio compared to traditional chemical reactors and enhanced heat transfer and mass transfer in the reduced dimensions of microchannels [15]. The process intensification benefits of micro process engineering for gas phase reactions [16–19] are consequently within focus of the world-wide research related to fuel processing for small and medium sized application.

In the present study, we have screened supported noble and base metal catalysts to decrease the CO concentration of the simulated methanol steam reforming reformate through the selective CO_x methanation at 150–350 °C and ambient pressure within an isothermal microchannel reactor. In addition, the effect of additional reactants such as steam and oxygen over Ni/CaO/Al_2O_3 catalyst was investigated and a distinct catalytic behaviour of Ni-based catalyst is presented, illustrating how gas phase molecules can dominate the reactivity and selectivity of surface reactions and regulate the switchover of the reaction paths for carbon oxide methanation reaction.

2. Experimental

2.1. Catalyst preparation

The microchannel sheets were coated with the respective catalysts to facilitate the appropriate chemical reactions. Two preparation methods may be applied to coat the catalysts (self-made or commercial) onto the microchannel surface.

The self-made catalyst coatings presented in this paper were exclusively based upon alumina carriers. Catalysts were prepared first by wash-coating alumina onto the microchannels. Therefore, the microchannels were filled manually with alumina carrier suspension and excess suspension was removed. The alumina suspension (20 wt.%) in deionized water contained also 5 wt.% polyvinyl alcohol (from Fluka) as a binder and 1 wt.% acetic acid. After drying at room temperature and calcination at a temperature of 600 °C in air, the alumina carrier coating was then impregnated with the desired amount of precursor (metal salt solutions). After drying, the coatings were calcined in air for 6 h at 450 °C. For checking purposes, the amount of the catalyst loaded onto the microchannel was then determined by measuring the weight gain after calcination. To coat the commercial catalyst, a direct wash-coating protocol (as already described above) with the commercial catalyst suspension was applied followed by an appropriate temperature treatment.

Details of this wash-coating procedure were described in our previous studies [20,21]. The deposited washcoats showed very good adhesion not only for fresh samples but also after application-oriented tests [22].

All the metal loadings of the catalysts in this context are based on weight percentage, i.e. wt.%. To make high performance micro-reactors, the inlet and outlet geometry of the micro-structured reactors was optimized by Computational Fluid Dynamics and numerical simulation to ensure the uniform flow distribution in the reactor.

2.2. Experimental set-up

The experimental apparatus consists of the feeding system, the microchannel reactor and the analysis section with an on-line gas chromatograph, which has been described in details elsewhere [23]. Gas mixtures required for the methanation reaction were regulated by the respective mass flow controllers (BRONKHORST HI-TEC). Water regulated by a liquid flow meter was vaporized by a laboratory scale evaporator (BRONKHOST CEM) and fed into the micro-reactor. CO and CO_2 methanation was carried out in a flow-type apparatus with a microchannel reactor at atmospheric pressure and a temperature range from 150 to 350 °C. The microreactor was powered by a heating cartridge regulated by a PID temperature controller with a K-type thermocouple inserted into the wall of the reactor. The

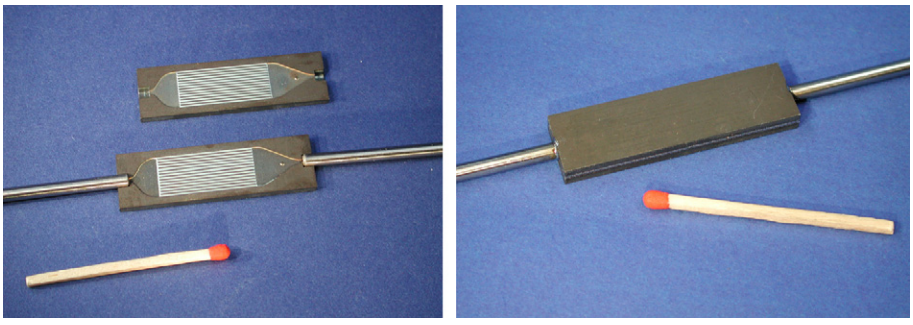

Fig. 1. Sandwiched microchannel reactor for methanation test. *Left*: coated platelets with capillary. *Right*: laser-welded reactor.

test reactor has a sandwich design with two micro-structured platelets being attached face to face (Fig. 1). The platelets carry 14 channels each 25 mm long, 500 μm wide and 250 μm deep. The channels together with the inlet and outlet zone were prepared by wet chemical etching. Each couple of platelets was coated with the individual carrier/catalyst and subsequently sealed by laser welding. Inlet and outlet capillaries were attached to the reactors by laser welding as well.

The methanation reaction was initiated by introducing simulated reformated gases equivalent to the product of methanol steam reforming with a total flow rate of 60 ml/min. The wash-coated supported catalyst (~20 μm thickness) was prereduced in 20% H_2/N_2 at 430 °C for 2 h prior to the catalytic test. The high heat transfer of the microstructured reactor avoids the formation of hot-spots and allows to perform gas phase reaction under isothermal condition. The composition of the reactor effluents were analyzed by an on-line ThermoFinnigan Trace gas chromatograph equipped with two thermal conductivity detectors. The analytical procedure allows for analysis of all species present in the reaction effluents including steam. Only methane was observed as a hydrogenated product in all measurements.

The conversion of CO was calculated by the following equation:

$$\text{CO conversion}\,(\%) = \frac{C_{\text{in(CO)}} - C_{\text{out(CO)}}}{C_{\text{in(CO)}}}$$

where $C_{\text{in(CO)}}$ and $C_{\text{out(CO)}}$ are the inlet and outlet concentration, respectively.

Selectivity reported in this study was estimated according to:

$$S_{\text{CO}} = \frac{C_{\text{in(CO)}} - C_{\text{out(CO)}}}{C_{\text{CH}_4}}$$

where C_{CH_4} is the methane concentration in the product.

Space time yield is calculated by methane yield obtained per unit time divided by the weight of the total catalyst.

2.3. Catalyst characterization

The specific surface area was determined by nitrogen sorption using a Sorptomatic 1990 (Carlo Erba Instruments) automatic apparatus and calculated by the BET method. X-ray measurements have been performed on catalyst samples in glass capillaries using a Siemens D5000 diffractometer with Cu Kα radiation in Debye–Scherrer geometry (capillary technique) and a position sensitive detector.

3. Results and discussion

It is well known that the catalytic methanation of carbon oxides proceeds effectively over various transition metal catalysts involving the following reactions:

$$\text{CO} + 3\text{H}_2 \rightarrow \text{CH}_4 + \text{H}_2\text{O} \quad (1)$$

$$\text{CO}_2 + 4\text{H}_2 \rightarrow \text{CH}_4 + 2\text{H}_2\text{O} \quad (2)$$

$$\text{CO}_2 + \text{H}_2 \rightarrow \text{CO} + \text{H}_2\text{O} \quad (3)$$

Eq. (1) is CO hydrogenation. Eq. (2) represents CO_2 methanation, the Sabatier reaction. Eq. (3) represents the reverse water-gas shift reaction. The major products of this process are CH_4 and H_2O. The application of PEMFCs requires high concentration of H_2 and low concentration of CO. Hence, the effect of reaction variables on selective CO methanation was performed to identify the appropriate operating conditions for the maximum CO methanation selectivity with minimum hydrogen loss owing to CO_2 methanation.

According to literature [24], methane production rates for noble metals decrease in the order Ru > Rh > Ir ~ Pd ~ Re. For base metals, the activity ranking is Ni > Co > Fe, with Ni more prone to methanation and Fe highly WGS selective. As a consequence, a series of Ru and Ni-based supported metal catalysts (Table 1) with high intrinsic methanation activity were synthesized with different metal loadings and promoters for the primary screening purpose and screened for methanation under realistic reformate conditions.

A preliminary screening of the catalytic performance of all prepared catalysts was carried out in terms of CH_4 formation rate and CO conversion. The CO conversion values are reported in Fig. 2 for Ru-based supported catalysts. Temperature dependence of the conversion of CO shows that catalytic activity varies with the metal loading, the type of support and surface area. CH_4 is only detectable at a temperature of at least 300 °C. 5 wt.% Ru/Al_2O_3 catalyst with higher surface area (184 m^2/g) is more active than 10 wt.% Ru/Al_2O_3 with lower BET surface area (115 m^2/g) catalyst. Yttrium-promoted Ru/ZrO_2 (5 wt.%) catalyst exhibits the poorest activity over the whole temperature range investigated. Nevertheless, all the prepared Ru-based catalysts show insufficient activity under current reaction conditions, among which the highest CO conversion is only 44% at 350 °C. As a comparison, the catalytic performance of Ni-based catalysts is presented in Fig. 3. Clearly, Ni-based catalysts show higher activity for selective methanation than the Ru-based catalysts. The catalytic behaviour of Ni-based catalyst is found to be remarkably dependent on the metal loading, the promoter and the type of support. The promoter-free Ni catalyst is inferior to the Mg-promoted Ni catalyst with the same metal loading, indicating that the basic dopants like Ca and Mg seem to have pronounced effect on activity for Ni-based catalysts. This finding seems to be contradictory to the suppressing effect of alkaline metals like Na and K in methanation activity [25]. Ni/Al_2O_3 is superior to Ni/TiO_2 catalyst with the identical

Table 1
Summary of tested catalysts

Catalysts	Ru/Al_2O_3	Ru/Al_2O_3	$Ru/Y/ZrO_2$	Ni/Al_2O_3
Metal loading [wt.%]	10	5	5	35
Surface area [m^2/g]	115	184	79	133
	$Ni/MgO/Al_2O_3$	$Ni/CaO/Al_2O_3$	Ni/TiO_2	Ni/TiO_2
Metal loading [wt.%]	35/4	43/6	35	10
Surface area [m^2/g]	117	88	75	62

The weight percentages for the various catalysts refer to the metal loadings without the carrier.

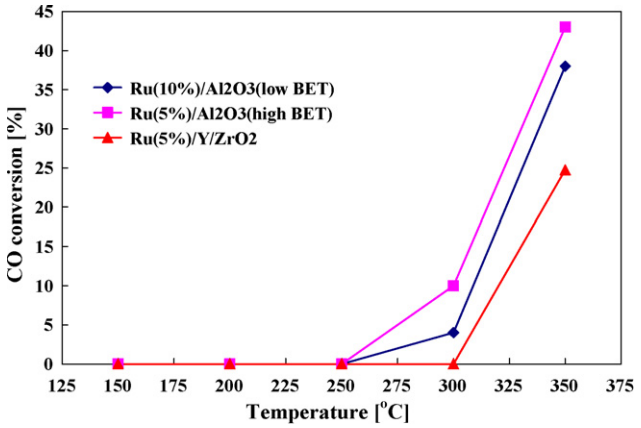

Fig. 2. Methanation activity over Ru-based catalysts. Feed composition (vol.%): H_2 (37.5), CO (1.6), CO_2 (12.5), H_2O (25), N_2 (balance gas); total flow rate 60 ml/min, $W/F = 0.333\ g_{cat}$ min/l.

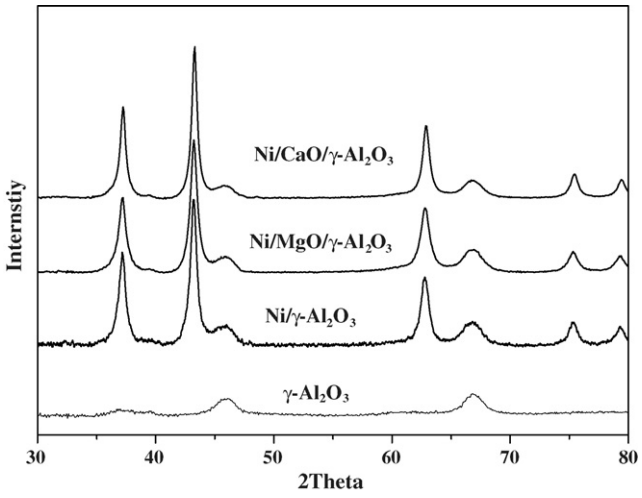

Fig. 4. XRD patterns of representative Ni-based catalysts.

metal loading, suggesting that an acidic support is a more appropriate catalyst carrier for methanation. The catalytic activity shows an increasing trend as the metal loading increases. The Ni/TiO_2 catalyst with the lowest metal loading (10 wt.%) is less active than the Ni/TiO_2 catalyst with the higher metal loading (35 wt.%). The $Ni/CaO/Al_2O_3$ catalyst with the highest metal loading (43 wt.%) was identified as the best methanizer as shown in Fig. 3, giving rise to the highest catalyst activity over the whole reaction temperature range. This result is in accordance with the previous studies revealing that higher Ni loadings favour the CO_x hydrogenation rate [26]. It is likely that Ni metal crystallites of relatively large size are suitable for the CO_x methanation. Similar results were reported by Van Meerten et al. [27].

Fig. 4 shows the X-ray diffraction patterns of some representative Ni-based catalyst specimens as-prepared. XRD patterns revealed sharp lines of good crystalline NiO phase for all Ni-containing catalysts. No lines of metallic nickel or other phases except NiO and Al_2O_3 were observed at all catalysts within the limits of accuracy. Given the low content of Ca/Mg present coupled with the similarities in the ionic radii of Ca^{2+}/Mg^{2+} with Ni^{2+}, it can be assumed that Ca and Mg become integrated into the solid structure of NiO or Al_2O_3.

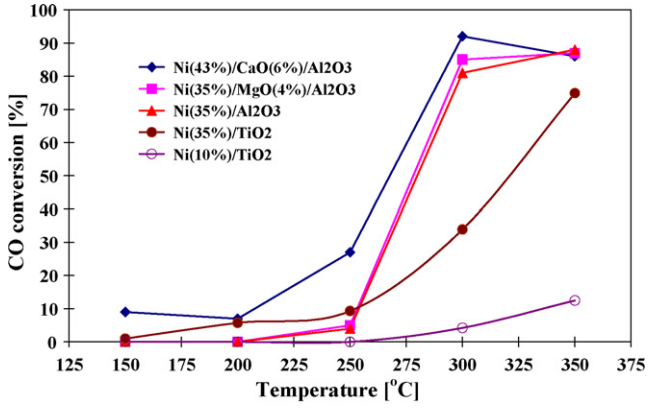

Fig. 3. Methanation activity over Ni-based catalysts. Feed composition: the same as those in Fig. 2.

The methanation was then carried out, respectively, over the best methanizer $Ni/CaO/Al_2O_3$ catalyst for solo-methanation (CO or CO_2 methanation) and comethanation (coexistence of CO and CO_2) in the absence of steam. The temperature dependence of CO conversion and CH_4 space time yield versus reaction temperature is shown in Fig. 5. Complete conversion of CO has been achieved at 300°C for CO solo-methanation. In comparing the methanation rates between CO_2 and CO, this study shows that the onset of CO_2 methanation occurs at 200 °C but at 250 °C for CO methanation. In agreement with the previous studies over Ni and Ni alloy catalysts [28,29], the CO_2 methanation activity is higher than that for CO over $Ni/CaO/Al_2O_3$ catalyst. In the coexistence of CO and CO_2, overall CH_4 formation rate is inhibited at lower temperature of 200 and 250 °C whereas it is accelerated at higher temperature of 300 and 350 °C in the presence of CO as compared to CO_2 solo-methanation, indicating the stronger adsorption of CO at relatively lower temperature. Compared with CO_2 methanation, it is evident that the cause of the enhancement in comethanation

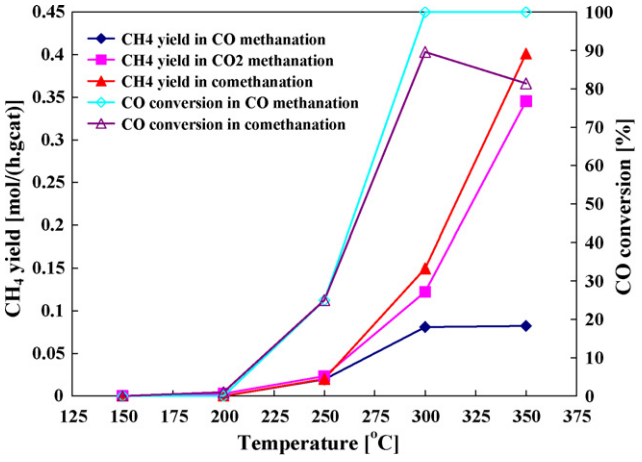

Fig. 5. Dry methanation activity over $Ni/CaO/Al_2O_3$ catalyst Feed composition (vol.%): CO methanation, H_2 (37.5), CO (1.6), N_2 (balance gas); CO_2 methanation, CO_2 (12.5), H_2 (37.5), N_2 (balance gas); comethanation, H_2 (37.5), CO (1.6), CO_2 (12.5), N_2 (balance gas); Total flow rate 60 ml/min), $W/F = 0.333\ g_{cat}$ min/l.

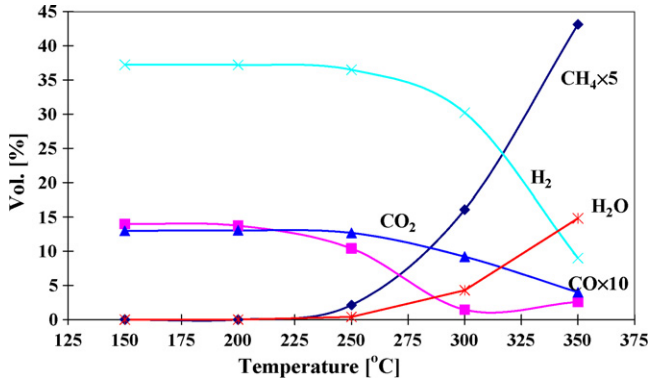

Fig. 6. Concentration profile of dry reformate methanation. Feed composition (vol.%): H_2 (37.5), CO (1.6), CO_2 (12.5), N_2 (balance gas).

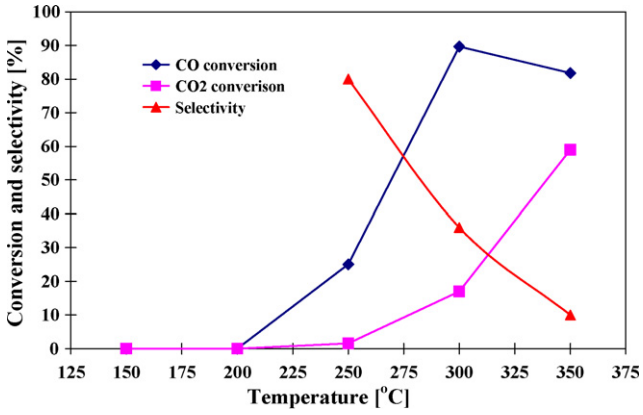

Fig. 7. Temperature dependence of CO and CO_2 conversion and H_2 selectivity in dry reformate methanation.

over $Ni/CaO/Al_2O_3$ catalyst is that CO_2 methanation is enhanced by the CO methanation in its higher conversion range. It is also found that CO and CO_2 were exclusively converted into CH_4. The C_2–C_4 selectivity below detection limitations indicates that this impregnated Ni catalyst lacks the carbon polymerization ability to produce larger hydrocarbons.

Fig. 6 shows the composition of the dry methanation off-gas with varying reaction temperature. In the dry reformate, CO concentration decreases at 250 °C at which methane is first detected in the off-gas while CO_2 concentration remains constant, suggesting the preferential methanation of CO at the relatively low temperature window from 250 to 300 °C. This is probably owing to the preferential adsorption of CO on the catalyst. The strong difference in the reactivity of surface formate by CO adsorption and carbonate by CO_2 adsorption species on Pt/ZrO_2 [30] is as follows. In the presence of hydrogen, formate results in methanation. On the other hand, carbonate decomposition brings about CO_2 formation. This also corroborates our conclusion of preferential CO methanation. Significant increase of methane formation was observed at the temperatures of 350 °C with the concomitant decrease of CO_2 concentration. At 350 °C, CO concentration increases again, probably due to the reversed water-gas-shift reaction, which is preferential at higher temperatures owing to the thermodynamic equilibrium. A further increase of methane formation is mainly attributed to the methanation of CO_2. As shown in Fig. 7, CO conversion starts with 25% at 250 °C and reaches the maximum of 89% at 300 °C. In contrast, CO_2 conversion starts up with 2% at 250 °C and increases continuously to 59% at 350 °C.

In the methanation of CO and CO_2, a considerable amount of water is formed according to Eqs. (1) and (2). Therefore, in order to assess the influence of the steam in realistic reformate on the reactivity and selectivity of the methanation, the methanation was also conducted with cofeeding of steam. The concentration profile of the reformate methanation product presented in Fig. 8 shows a similar pattern compared to that obtained in dry methanation but different in a significant extent in terms of the reactivity and selectivity. The overall methanation rate is retarded by the presence of water. The inhibited methanation rate is attributed to kinetic limitations brought about by the excess of steam in the feed. In spite of inhibition effect of steam on methanation rate, CH_4 formation contributed from CO methanation significantly improves in the presence of steam though the origin for this remains unclear so far. As shown in Fig. 9, CO_2 conversion remains zero at a temperature lower than 250 °C and the onset of CO_2 methanation occurs at 300 °C with a CO_2 conversion of 12%, indicating a highly selective CO methanation at lower temperature. It was found that 100% selective CO methanation is possible for simulated reformate, provided the reaction

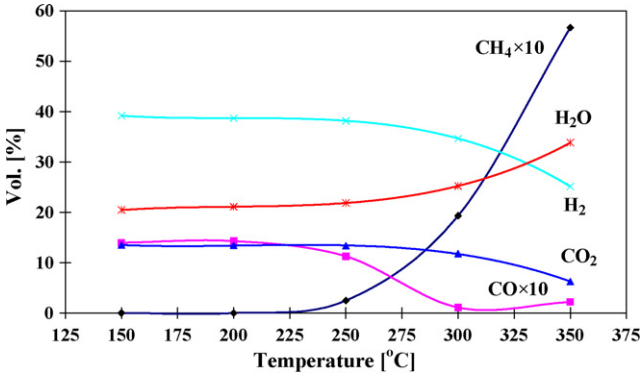

Fig. 8. Concentration profile of simulated reformate methanation. Feed composition: the same as those in Fig. 2.

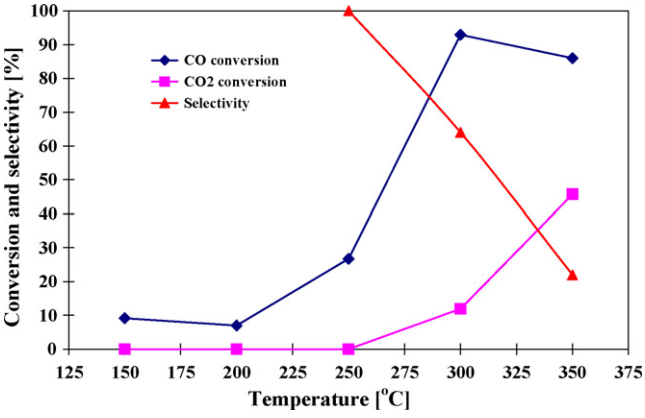

Fig. 9. Temperature dependence of CO and CO_2 conversion and H_2 selectivity in simulated reformate methanation.

temperature is controlled to be lower than a critical temperature, e.g. 250 °C in this study. This conclusion is in accordance with the results obtained from Ru-based catalyst in conventional fixed-bed reactor, despite that the fact that contact time in conventional reactor is much greater than that used in this study [31]. Ni/ZrO_2 was reported to be effective catalyst for complete removal of CO through the methanation in conventional fixed-bed reactor under the similar space velocity to this study [13]. Nevertheless, CO and steam content are quite low compared to the values used in this study. In comparison to the result in the presence of steam, CO methanation selectivity is only 80% in the absence of steam at 250 °C. The selectivity of CO methanation decreases to 64% and 22% as the reaction temperature further increases to 300 and 350 °C, respectively.

Fig. 10 shows the concentration profile change by variation of reaction temperature when gaseous oxygen is added to the feed. In contrast to the published promoting role of gas phase oxygen additive in catalytic methanation over Ru-based catalyst [14], this study evidences that the methanation pathway over $Ni/CaO/Al_2O_3$ catalyst can be profoundly influenced by the ambient oxygen addition. In the presence of oxygen, the CO concentration in the low temperature window of 150–200 °C is significantly smaller than in the absence of oxygen. Meanwhile CO_2 concentration is slightly higher than its inlet concentration, indicating CO oxidation (Eq. (4)) occurs at the low temperature. Moreover, in the presence of oxygen, the water content at the low temperature is much higher than its concentration without oxygen additive, implying the occurrence of hydrogen oxidation (Eq. (5)). With the rise of temperature up to 250 and 300 °C, the increasing CO content and continuous conversion of hydrogen into water demonstrate that hydrogen combustion prevails over CO oxidation and consumes most of the oxygen. It is obvious that methanation only starts directly after the complete consumption of gas phase oxygen at 350 °C.

$$2CO + O_2 \rightarrow 2CO_2 \quad (4)$$

$$2H_2 + O_2 \rightarrow 2H_2O \quad (5)$$

To examine the validity of this assumption, investigations were also performed in the solo-methanation of CO and CO_2

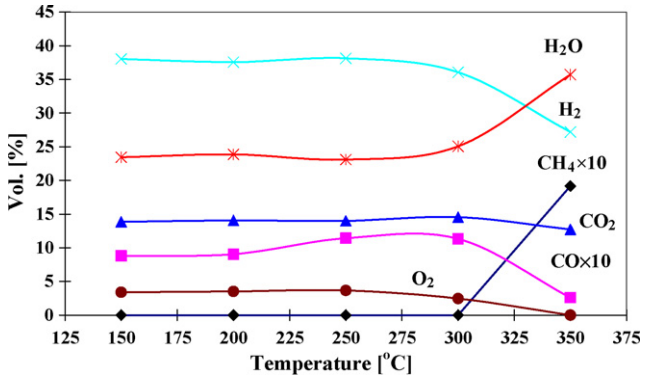

Fig. 10. Concentration profile of simulated reformate methanation with oxygen addition in the feed. Feed composition (vol.%): O_2 (4.8); rest, the same as those in Fig. 2.

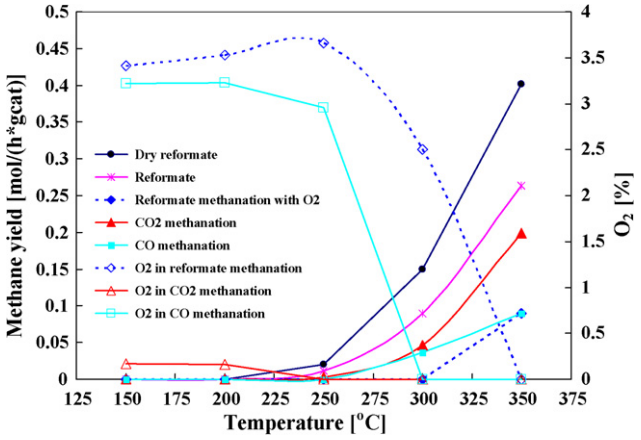

Fig. 11. The influence of gas additive on methane yield. Feed composition (vol.%): simulated reformate methanation with O_2, O_2 (4.8); CO_2 methanation, O_2 (4.8); CO methanation, O_2 (4.8); balance gas N_2; the rest, the same as those in Fig. 2. *Symbols*: solid, methane yield; open, oxygen content).

with O_2 additive. The methane space time yield and oxygen volume percentage in off-gas under comethanation and solo-methanation were also plotted in Fig. 11. The regulation effect of the gaseous oxygen on the methanation rate is also evidenced by the solo-methanation of CO and CO_2 in the presence of oxygen. With the addition of oxygen, the methane space time yield follows the order: CO_2 methanation > CO methanation > reformate methanation. Specifically, the oxygen content in CO_2 methanation declines to 0.2% in the off-gas effluent at a temperature as low as 150 °C. In contrast, oxygen consumption is largely suppressed due to the presence of CO for CO and reformate methanation. Although the catalyst exhibits different catalytic behaviour, depending on the feed compositions, the consistent observation is that methanation only occurs after the complete consumption of gas phase oxygen at 250, 300, and 350 °C for CO_2, CO, and reformate methanation, respectively.

The role of gas phase molecules in surface catalytic reactions [32] has to be considered for the switchover of the reaction pathway on $Ni/CaO/Al_2O_3$ catalyst in the presence of gaseous oxygen. From a thermodynamical point of view, while the methanation of carbon oxides is thermodynamically feasible, total combustion to CO_2 and water is more energetically favourable in the presence of gaseous oxygen, so methanation can only occur upon complete consumption of gaseous oxygen. From mechanistic considerations, the presence of gaseous oxygen leads to oxidation or high oxygen coverage of the Ni surface and the products associated with total combustion, namely, CO_2 and water, are observed on the oxidized Ni surface (Ni^{2+}) [33], as gaseous oxygen is present. It was established that methanation over Ni-based catalyst occurs predominantly by the direct hydrogenation of the surface carbon species on reduced form of Nickel (Ni^0) [34,35]. The reaction pathway for the formation of crucial methanation intermediate, i.e. surface carbon species, is probably cut off due to the presence of oxygen. On the other hand, the experimental result has indicated that the chemisorbed hydrogen, in the presence of gaseous oxygen, exclusively reacts with surface oxygen species to form water and consequently the hydrogenation of surface carbon species, even

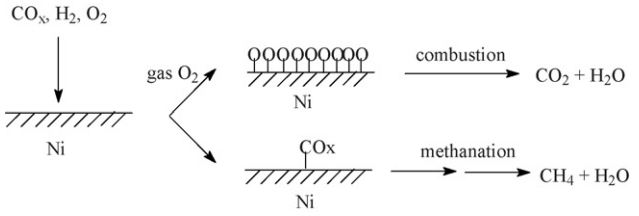

Fig. 12. Switchover of the methanation pathway in the presence of gaseous oxygen over Ni-based catalyst.

if they are formed under an oxidative atmosphere, is totally blocked. It is suggested that the Ni^0 sites are responsible for the methanation. Not only must there be a proper balance between Ni^0 and oxygen coverage on the surface, but also the reactivity of the adsorbed oxygen atoms on the Ni or NiO catalyst surface controls the reaction pathway: on reduced Ni surface the adsorbed oxygen species do not catalyze H_2 and CO oxidation, but on NiO or Ni with high oxygen coverage they readily oxidize CO and H_2 (see Fig. 12). Once the gaseous oxygen is completely consumed, Ni catalyst surface is altered to its reduced state which is catalytically active for methanation due to the dynamic interplay of the reactants and catalyst surface. The different behavior of Ni and Ru-based supported catalyst is most likely due to their different chemical nature and surface reactivity enhanced at the high oxygen coverages.

4. Conclusion

Selective removal of CO by methanation of carbon oxides has been conducted over wash-coated supported metal catalysts in a microchannel reactor with simulated reformate feeding. The primary catalytic screening over a series of Ru and Ni-based catalysts shows that methanation activity is markedly dependent on the type of metal and carrier, metal loading, and promoter. The catalytic evaluation of the best methanizer Ni/CaO/Al_2O_3 in this study was carried out under conditions with different feed compositions, the solo-methanation or comethanation, methanation in the presence or absence of steam. The experiments demonstrate that the microchannel reactor is an excellent tool for studying the reaction pathway by varying feed composition and reaction temperature. The critical temperature for selective methanation was identified to be 250 °C below which preferential CO methanation occurs. The inhibiting role of steam on methanation rate was demonstrated. This work also presents the catalytic behavior of $Ni/CaO/Al_2O_3$ catalyst which is different from a Ru-based catalyst in a microchannel reactor, showing that the carbon oxides methanation pathway, i.e. catalytic selectivity on $Ni/CaO/Al_2O_3$ catalyst is regulated by the gas phase oxygen. The switchover of the combustion reaction in the presence of gas phase oxygen to methanation in the absence of gas phase oxygen accounts for the role of ambient oxygen and is explained by a dynamic change of the catalyst surface and changeable surface oxygen reactivity dominated by the gas phase oxygen.

Acknowledgements

This work is funded by the ‘‘Rheinland-Pfalz Stiftung für Innovation’’ under project ‘‘COMPELL-Gassensorik für die Prozesskontrolle in Brennstoffzellen-Systemen mit integrierter Brenngaserzeugung’’.

References

[1] G. Hoogers, Fuel Cell Technology Handbook, CRC Press, 2002.
[2] R. Moy, Science 301 (2003) 47.
[3] D.L. Trimm, Z.I. Önsan, Catal. Rev. Sci. Eng. 43 (2001) 31.
[4] F. Joensen, J.R. Rostrup-Nielsen, J. Power Sources 105 (2002) 195.
[5] S.H. Oh, R.M. Sinkevitch, J. Catal. 142 (1993) 254.
[6] D.L. Trimm, Appl. Catal. A 296 (2005) 1.
[7] R.W. McCabe, P.J. Mitchell, Catalysis 103 (1987) 419.
[8] G. Kolb, V. Hessel, V. Cominos, C. Hofman, H. Löwe, G. Nikolaidis, R. Zapf, A. Ziogas, E.R. Delsman, M.H.J.M. de Croon, J.C. Schouten, O. de la Iglesia, J. Santamaria, Catal. Today 120 (2007) 2.
[9] A. Luengnaruemitchai, S. Osuwan, E. Gulari, Int. J. Hydrogen Energy 29 (2004) 429.
[10] W.L. Deng, J.D. Jesus, H. Saltsburg, M. Flytzani-Stephanoloulos, Appl. Catal. A 291 (2005) 126.
[11] G.A. Somojai, Introduction to Surface Chemistry and Catalysis, Wiley, New York, 1994.
[12] Y. Borodko, G.A. Somojai, Appl. Catal. A 186 (1999) 355.
[13] S. Takenaka, T. Shimizu, K. Otsuka, Int. J. Hydrogen Energy 29 (2004) 1065.
[14] O. Görke, P. Pfeifer, K. Schubert, Catal. Today 110 (2005) 132.
[15] V. Hessel, S. Hardt, H. Löwe, Chemical Micro Process Engineering—Fundamentals, Modelling and Reactions, Wiley-VCH, 2004.
[16] V. Hessel, H. Löwe, A. Müller, G. Kolb, Chemical Micro Process Engineering—Processing and Plants, Wiley-VCH, 2005.
[17] G. Kolb, V. Hessel, Chem. Eng. J. 98 (2004) 1.
[18] L. Kiwi-Minsker, A. Renken, Catal. Today 110 (2005) 2.
[19] G. Markowz, S. Schirrmeister, J. Albrecht, F. Becker, R. Schütte, K.J. Caspary, E. Klemm, Chem. Eng. Technol. 28 (2005) 459.
[20] G. Kolb, R. Zapf, V. Hessel, H. Löwe, Appl. Catal. A 277 (2004) 155.
[21] R. Zapf, C. Becker-Willinger, K. Berresheim, H. Bolz, H. Gnaser, V. Hessel, G. Kolb, P. Löb, A.K. Pannwitt, A. Ziogas, Chem. Eng. Res. Des. Trans. IChemE Part A 81 (2003) 721.
[22] R. Zapf, G. Kolb, H. Pennemann, V. Hessel, Chem. Eng. Technol. 29 (2006) 1.
[23] G. Kolb, H. Pennemann, R. Zapf, Catal. Today 110 (2005) 121.
[24] F. Solymosi, A. Erdohelyi, J. Mol. Catal. 8 (1980) 471.
[25] K. Yaccato, R. Carhart, A. Hagemeyer, A. Lesik, P. Strasser, A.F. Vole Jr., H. Turner, H. Weinberg, R.K. Grasselli, C. Brooks, Appl. Catal. A 296 (2005) 30.
[26] A.E. Aksoylu, Z.I. Önsan, Appl. Catal. A 164 (1997) 1.
[27] R.Z.C. Van Meerten, A.H.G.M. Beaumont, P.F.M.T. Van Nisselrooij, J.W.E. Coenen, Surf. Sci. 135 (1983) 565.
[28] T. Inui, M. Funabiki, M. Suehiro, T. Sezume, J. Chem. Soc. Faraday Trans. 75 (1979) 787.
[29] T. Inui, M. Funabiki, Chem. Lett. 251 (1978).
[30] H. Kalies, N. Pinto, G.M. Pajonk, D. Bianchi, Appl. Catal. A 202 (2000) 197.
[31] G. Xu, X. Chen, Z.G. Zhang, Chem. Eng. J. 121 (2006) 97.
[32] Y. Iwasawa, Acc. Chem. Res. 30 (1997) 103.
[33] D. Dissanayake, M.P. Rosynek, K.C.C. Kaharas, J.H. Lunsford, J. Catal. 132 (1991) 117.
[34] M. Araki, V. Ponec, J. Catal. 44 (1976) 43.
[35] S. Fujita, M. Nakamura, T. Doi, N. Takezawa, Appl. Catal. A 104 (1993) 87.